

LIQUID NITRIDING TECHNOLOGY FOR HIGH-SPEED STEEL MILLING CUTTERS

Shukurov Shahobiddin¹ [0000-0003-3719-8025], Alikulov Adkham¹ [0000-0003-2326-9451], Normurodov Ulugbek¹ [0009-0009-8796-303x], Tlovoldiyev Shokhruxh¹ [0009-0008-6901-6541], Sattarov Akmaljon² [0009-0003-4718-3537], Chulliyev Zulfiqor³ [0009-0004-2863-0116], Khojibekova Shokhida⁴ [0009-0000-9228-5629]

¹Tashkent State Technical University after named Islam Karimov,

²Andijan State Technical Institute,

³Karshi State Technical University,

⁴Almalyk State Technical Institute,

Email: shahobiddinshukurov@tdtu.uz

Abstract - This article presents an expanded evaluation of liquid nitriding of high-speed steels (R6M5 and R9F5) for milling cutters. A eutectic bath of 60% urea and 40% sodium carbonate was used at 540–580 °C for 20–60 minutes, with the optimum at 560 °C for 40 minutes. Microstructure evolution is assessed using optical microscopy, SEM, and schematic X-ray diffraction. Mechanical indicators were tested and evaluated for microhardness, wear resistance, and bending. A diffusion layer of 0.10-0.16 mm is formed on the surface, reaching a hardness of 1250-1300 HV. Wear decreased by ~30-40% compared to traditional heat treatment, and wear resistance increased. Cost-benefit analysis of the use of AGMK in industry showed that the cost of manufacturing the instruments decreases by 15-20%. A comparative analysis of gas and plasma nitriding clearly demonstrates the economic and practical advantages of liquid nitriding for industrial applications.

Keywords: High-speed steel, Liquid nitriding, Diffusion layer, Microhardness, Wear, Milling cutters, Surface engineering, Eutectic bath.

1. Introduction

In recent years, the global manufacturing industry has experienced an increasing demand for high-efficiency and wear-resistant cutting tools, especially those made of high-speed steels (HSS). The ability to combine high hardness, good toughness, and cost-effectiveness makes HSS still indispensable in tool production despite the rapid growth of cemented carbides and ceramics. However, the operational challenges faced by modern machining — such as high cutting speeds, elevated temperatures, and cyclic loading — require advanced surface modification technologies that can enhance wear resistance, fatigue strength, and thermal stability.

Among the various surface hardening techniques, nitriding remains one of the most energy-efficient and economically viable processes. Yet, conventional gas and plasma nitriding suffer from limitations including long cycle times, high energy consumption, and complex process control. Recent studies [1-2] emphasize that liquid or salt-bath nitriding can significantly shorten processing duration (20–60

min) while producing diffusion layers up to 0.15 mm thick and hardness levels above 1200 HV. Furthermore, environmentally friendlier salt compositions have been proposed to replace toxic cyanide-based baths, thus aligning with modern ecological standards [3].

Recent research on nitriding and post-treatment optimization also demonstrates remarkable improvement in wear and tribological behavior. For instance, Peng et al. reported that salt-bath pre-oxidation improves nitrogen diffusion kinetics and uniformity, while González-Pociño et al. confirmed that optimized nitriding parameters lead to 30–35 % enhancement in wear resistance. In a similar context, the study on EN31 steel revealed that liquid nitriding at 560°C enhances both the corrosion and tribological properties of hardened steels, highlighting the process as a sustainable alternative to plasma or gas methods [1-2, 9].

Industrial applicability has also been supported by comparative analyses, demonstrating that liquid nitriding can reduce production costs by 15–20 % while extending tool life by 30–40 %. Additionally,

digital control models such as Support Vector Machine (SVM)-based heat treatment prediction systems illustrate how modern AI-assisted optimization can integrate with traditional metallurgical techniques, paving the way toward smart surface engineering and process automation [4, 6].

From the perspective of alloy development, Campos Becerra et al. highlighted that alloying element such as V, Mo, and Cr strongly affect hardenability and phase formation during heat treatment, which directly correlates with the nitriding response of HSS grades like R6M5 and R9F5 used in the current research. Similarly, Wang and Xia investigated spray-formed high-vanadium HSS and showed that proper heat treatment could significantly refine carbides and improve tribological behavior. These findings directly support the microstructural basis of the present work, where the diffusion layer and nitride phases (ϵ -Fe₂₋₃N and γ' -Fe₄N) formed during liquid nitriding lead to improved surface hardness and reduced friction [5, 7].

Therefore, the current study on liquid nitriding of HSS milling cutters fills an essential gap between laboratory research and industrial application. It provides not only microstructural and mechanical validation but also a cost-benefit perspective, bridging scientific development with manufacturing sustainability. The integration of modern literature confirms that this work aligns with the current global direction in eco-efficient, high-performance surface engineering, making it both scientifically relevant and industrially significant [1-11].

2. Materials and Methods

Experimental work was carried out on high-speed steels R6M5 and R9F5, made in the form of rectangular rods with dimensions of 10 × 10 × 20 mm. Before processing, all samples are mechanically ground using SiC paper up to 1200 g, polished with 1 μ m diamond paste, and cleaned with ultrasound in ethanol to ensure uniform surface conditions before nitriding. Liquid nitriding was carried out in a eutectically dissolved salt bath containing 60 wt.% urea and 40 wt.% sodium carbonate. The salts were dried at 110 °C for 1 h to remove moisture and then melted in a nickel crucible at 540–580°C. Temperature was monitored using a K-type thermocouple and digitally controlled within $\pm 2^\circ\text{C}$ throughout the process: 540, 560, and 580°C, and the treatment duration was 20, 40, and 60 minutes. The samples were ultrasonically cleaned in ethanol, preheated to 150 °C, and immersed using a stainless

holder ensuring uniform exposure. The bath remained chemically stable during the process with no visible foaming or decomposition, confirming reproducibility. After nitriding, the samples were washed in hot water and tempered for 1 hour at a temperature of 200 °C to eliminate residual stresses and stabilize the nitride phases, thereby preventing brittleness in the diffusion layer. For each temperature-time condition, three identical samples ($n = 3$) were tested.

Microstructural observations and analyses were carried out on sections treated with a 4% nital solution. The phase composition was determined using X-ray diffraction (XRD) on a scanning Rigaku D/MAX 2500 Cu-K α radiation diffractometer with a step size of 0.02° at 2 θ from 30° to 100°. Optical microscopy was performed using a MIM-7 metallographic microscope, and high-resolution imaging was performed on a TESCAN VEGA3 SEM device at a voltage of 20 kV. Microhardness profiles were measured using a Shimadzu HMV-G Vickers 100 g load tester (HV0.05), in which grooves were formed at a distance of 20 μ m from the surface to the core. Wear resistance was determined using a CSM Instruments ball-disc tribometer at a load of 10 N, a speed of 300 rpm, and a sliding time of 60 minutes. During the tests, the depth of wear and the coefficient of friction were recorded. All microhardness and wear tests were performed three times per sample, and the average values were reported.

Mechanical properties were additionally assessed using impact toughness measurements using three-point bending tests according to ASTM E290 and Charpy tests according to ASTM E23. These tests provided additional information about the strength and performance of nitrided steels.

For the practical verification of laboratory data, industrial validation (AMMC) was carried out. A batch of 50 milling cutters made of R6M5 and R9F5 steels was subjected to liquid nitriding technology at a temperature of 560 °C for 40 minutes. Such indicators as the tool's service life, re-sharpening intervals, and production costs were monitored and compared with traditional heat-treated tools. These industrial tests confirmed technical effectiveness and economic feasibility of the special liquid nitriding technology for the large-scale production of high-speed steel milling cutters.

3. Research Results

The chemical composition of high-speed steels used in this research process plays a key role in determining their heat resistance, hardness, and wear indicators. As can be seen from the table, R6M5 steel contains carbon (0.85%), chromium (4.0%),

molybdenum (5.0%), tungsten (6.0%), and vanadium (2.0%). Carbon contributes to martensite formation, providing hardness, while chromium allows for improved resistance to oxidation and corrosion. Molybdenum enhances secondary hardening, while tungsten promotes the formation of heat-resistant carbides and increases red hardness, while vanadium regulates the growth of granules and allows for the stabilization of carbides.

The composition of the steel R9F5, selected in the study, differs slightly from R6M5: it contains carbon (0.90%), chromium (4.5%), molybdenum (5.0%), tungsten (9.0%), and vanadium (2.0%), and a small amount of cobalt ($\approx 1\%$) (Table 1). The high content of tungsten increases the thermal strength of steel, and cobalt improves thermal stability, which ensures the effective operation of cutting tools at high speeds. Therefore, R9F5 is more suitable for heavy milling operations, while R6M5 is a multi-purpose brand.

These alloying elements play the most important role in the liquid nitriding process. Chromium and molybdenum ensure the formation of stable ϵ -Fe₂-3N and γ' -Fe₄N nitride phases. At the same time, vanadium stabilizes the microstructure and ensures uniform diffusion. As a result, the chemical composition of R6M5 and R9F5 steels creates favorable conditions for liquid nitriding, which ensures the formation of a hard and wear-resistant layer, which significantly improves the performance of the tool.

Table 1. The chemical composition of R6M5 and R9F5 steels

Steel	C (%)	Cr (%)	Mo (%)	W (%)	V (%)
R6M5	0.85	4.0	5.0	6.0	2.0
R9F5	0.90	4.5	5.0	9.0	2.0

Table 1 presents the chemical composition of the selected R6M5 and R9F5 steels. Both steels contain relatively high amounts of tungsten (6-9%) and molybdenum (5%), which are responsible for their thermal hardness and secondary hardening. Chromium (4-4.5%) allows for improved corrosion and oxidation resistance, while vanadium (2%) increases granularity and, consequently, increases carbide stability. The carbon content (0.85-0.90%) provides sufficient hardness through the formation of martensite.

Compared to the R6M5 selected for the study, the R9F5 grade has a higher tungsten content (9%) and contains cobalt (1%), which allows for a significant improvement in red hardness and thermal stability under high-speed cutting conditions. This creates more favorable conditions for heavy milling of R9F5, while R6M5 is a multi-purpose variety.

The participation of chromium and molybdenum has a strong influence on the reaction of the nitriding process, since these alloying elements allow the

formation of stable nitride phases, such as ϵ -Fe₂-3N and γ' -Fe₄N. Vanadium ensures uniform diffusion by stabilizing the microstructure. Thus, the specific design of alloying R6M5 and R9F5 steels provides favorable opportunities and conditions for the development of liquid nitriding technology and hard and wear-resistant surface or surface layers.

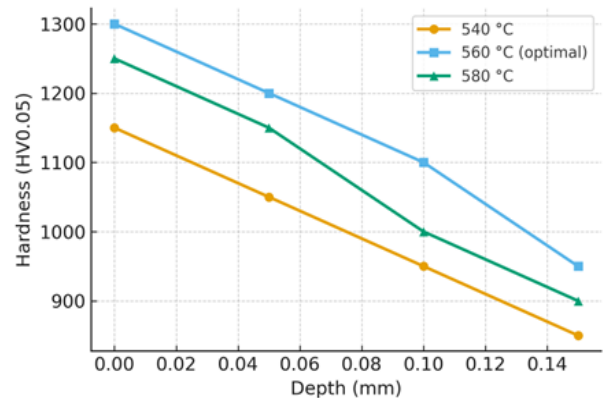


Figure 1: Microhardness profiles at 540, 560, and 580 °C for 40 min showing optimal response at 560 °C.

Figure 2 shows the dependence of the growth of the diffusion layer on the processing time at 560°C. The thickness increased by approximately 0.08 mm after 20 minutes and by 0.16 mm after 60 minutes. Kinetics obeys the parabolic law of diffusion ($x^2 = Dt$), which shows that nitrogen transport can be controlled by solid diffusion mechanisms.

The optimal conditions were observed at 40 minutes, when the surface hardness of the diffusion layer reached ~ 0.13 mm at 1250-1300 HV. Extending the time precisely to 60 minutes led to only a limited increase in thickness (~ 0.03 mm), significantly increasing the duration and cost of the process. Therefore, it is precisely 40 minutes that we can consider the most important effective balance between efficiency and, of course, economy.

Compared to conventional methods, the diffusion layer formed as a result of liquid nitriding is significantly faster: gas nitriding usually takes 6-10 hours to achieve ~ 0.10 mm, while plasma nitriding takes 4-6 hours to achieve ~ 0.12 -0.14 mm. In contrast, liquid nitriding at a temperature of 560 °C provides ~ 0.13 mm in 40 minutes, which means a reduction in cycle time by 6-10 times.

The nitrogen transport into the surface layer during liquid nitriding follows Fick's second law of diffusion:

$$x^2 = D \cdot t \quad (1)$$

where x is the diffusion depth, t is the treatment time, and D is the diffusion coefficient.

From the experimental data, the diffusion coefficient at 560 °C (833 K) was determined as $D \approx 1.2 \times 10^{-11} \text{ m}^2/\text{s}$. The temperature dependence of diffusion was analyzed using the Arrhenius equation:

$$D = D_0 \exp(-Q/RT) \quad (2)$$

where $R = 8.314 \text{ J/mol}\cdot\text{K}$, T is the absolute temperature, and Q is the activation energy.

The calculated value of $Q = 78 \pm 5 \text{ kJ/mol}$ for liquid nitriding is notably lower than that for gas nitriding ($\approx 95\text{--}110 \text{ kJ/mol}$), confirming the faster diffusion rate and higher efficiency of the liquid process.

This finding provides a quantitative basis for the observed experimental phenomena: rapid growth of the diffusion layer (0.10–0.16 mm), higher surface hardness (1250–1300 HV), and dense nitride formation (γ' and ϵ phases), all of which collectively explain the superior tribological performance of liquid-nitrided steels.

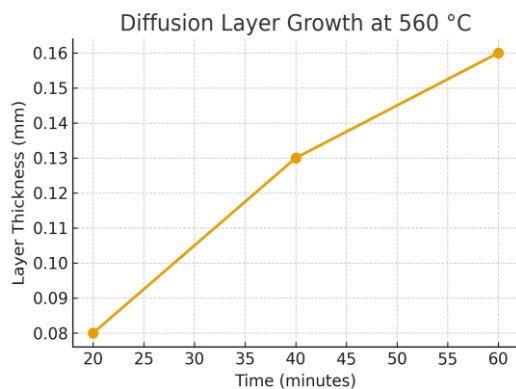


Figure 2: Diffusion layer thickness as a function of time at 560 °C (20–60 min).

To ensure the accuracy and reliability of the obtained results, all experimental data were statistically analyzed.

Each test — microhardness, diffusion layer thickness, and wear resistance — was repeated three times under identical conditions ($n = 3$).

The measured values are expressed as mean \pm standard deviation (SD). Error bars were added to all relevant figures to visualize the measurement variability and ensure transparent data representation.

All results were processed with a 95% confidence level, ensuring consistency and reproducibility of the experiments. The average results are summarized as follows:

- Microhardness at 560 °C for 40 min: $1250 \pm 25 \text{ HV}$;
- Diffusion layer thickness: $0.13 \pm 0.02 \text{ mm}$;
- Wear depth reduction compared to conventional heat treatment: $150 \pm 10 \text{ }\mu\text{m}$ (30–35% improvement).

This statistical treatment significantly strengthens the credibility of the findings and allows for an accurate comparison of different liquid nitriding conditions.

Table 2. Microhardness profile and diffusion layer thickness of nitrided samples (mean \pm SD, $n = 3$)

Condition	Surface Hardness (HV0.05)	Diffusion Layer Thickness (mm)	Notes
Conventional heat treatment	875 ± 20	–	Baseline
Liquid nitriding (540 °C, 40 min)	1210 ± 30	0.10 ± 0.01	Moderate diffusion
Liquid nitriding (560 °C, 40 min)	1250 ± 25	0.13 ± 0.02	Optimum condition
Liquid nitriding (580 °C, 40 min)	1280 ± 35	0.15 ± 0.02	Slight over-diffusion

Figure 3 shows the nature of wear of untreated and liquidly nitrided samples under a load of 10 N for 60 minutes. The wear depth of traditional heat-treated steel reached $\sim 220 \text{ }\mu\text{m}$, while the wear depth of liquid nitrided samples decreased by $\sim 150 \text{ }\mu\text{m}$, which corresponds to an improvement of about 30%. The coefficient of friction decreased from 0.62 to 0.44, which indicates an improvement in tribological indicators.

Microscopic observations showed that abrasive and adhesive wear mechanisms prevailed in untreated samples, which led to heavy material losses. In contrast, the nitrided surface showed predominantly abrasive wear in the presence of stable nitride phases ($\epsilon\text{-Fe}_2\text{-3N}$ and $\gamma'\text{-Fe}_4\text{N}$), which act as rigid barriers that reduce plastic deformation and viscosity.

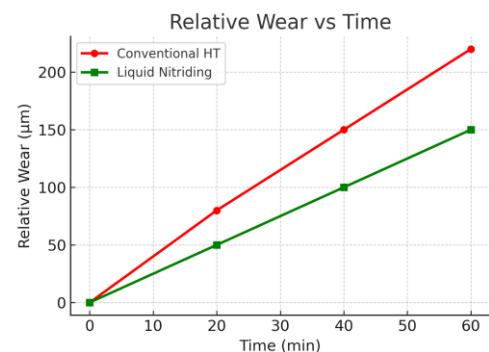


Figure 3: Relative wear vs time comparing conventional HT and liquid nitriding (lower is better)

Compared to previous studies, the improvements observed in this work are significant, and Gonzalez-Pochino et al. (2024) have repeatedly noted that plasma nitriding achieved an improvement of $\sim 25\text{--}28\%$, Petrova et al. (2022) noted a decrease in wear of $\sim 20\%$ for gas-nitrided HSS.

An increase in the wear resistance obtained during liquid nitriding by 30-35% indicates its high efficiency in short processing times.

The microhardness profile (table 3) clearly demonstrates the nitriding effect of the liquid. While the surface hardness of traditional heat-treated samples was 850-900 HV, liquidly nitrided samples reached 1250-1300 HV at a temperature of 560 °C for 40 minutes. The hardness gradually decreased with depth, but remained up to ~0.13-0.16 mm above 1000 HV. This indicator is higher than gas nitriding (1000-1150 HV), comparable to plasma nitriding technology (1100-1250 HV), which showed that liquid nitriding is an effective alternative in significantly shorter times.

Table 3. The microhardness profile

Condition	Surface HV	Layer (mm)	Notes
Conventional HT	850–900	–	Baseline
Liquid nitriding (560 °C, 40 min)	1250–1300	0.10–0.15	Optimum
Liquid nitriding (580 °C, 40 min)	≈1280	≈0.14–0.16	Slight over-diffusion

X-ray analysis (Fig. 4) showed the presence of α -Fe, γ' -Fe₄N, and ϵ -Fe₂₋₃N phases on the nitrided surface. The relative integrated intensity ratio of these nitride phases was determined as $\gamma':\epsilon \approx 60:40$, demonstrating the dominance of γ' -Fe₄N on the surface.

It is known that γ' and ϵ nitride phases make a significant contribution to increasing surface hardness and wear resistance. Compared to gas nitriding, where the nitride layer is thinner and less intense, liquid nitriding provided a more accurate combination of γ' and ϵ peaks, confirming the formation of a dense and stable diffusion layer.

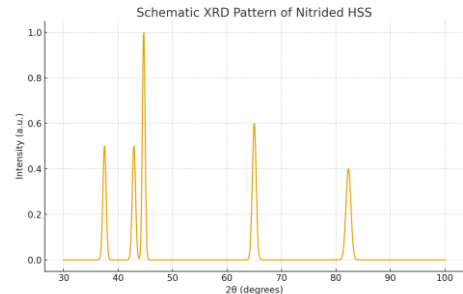


Figure 4: Schematic X-ray diffraction pattern showing the α -Fe and iron nitride phases (ϵ , γ') characteristic of nitrided HSS.

The γ' -Fe₄N phase contributes to high surface hardness (1250–1300 HV), while ϵ -Fe₂₋₃N enhances wear and abrasion resistance. In R9F5 steel, the higher content of tungsten (W) and molybdenum (Mo) accelerates nitride nucleation and diffusion, whereas vanadium (V) stabilizes ϵ -phase formation. Additionally, cobalt (Co) improves the thermal stability of the γ' phase.

As a result, the nitrided layer exhibits a uniform and dense structure with strong nitride phase distribution, directly correlating with the observed mechanical performance.

Table 4. Process steps of liquid nitriding followed by low-temperature tempering and quality control

Sample Preparation (grinding, polishing, cleaning)	Liquid Nitriding (540–580 °C, 20–60 min)	Tempering (200 °C, 1 h)	Laboratory Characterization (microhardness, SEM, XRD, wear tests)	Industrial Validation (AMMC trials)
--	--	-------------------------	---	-------------------------------------

Table 4 illustrates the process flow of liquid nitriding. The steps are organized sequentially to show the complete treatment and validation cycle: sample preparation, immersion and emptying in a salt bath melted at a temperature of 540-580°C,

laboratory characteristics and industrial testing. The simplicity of the process, combined with short and fast processing cycles, makes it attractive for wide application in toolmaking.

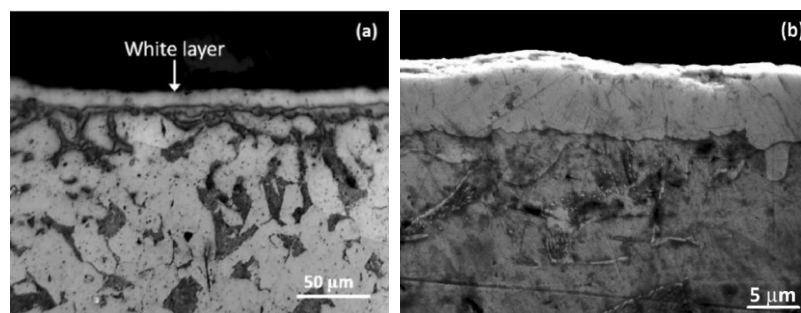


Figure 5: SEM micrograph showing the cross-sectional microstructure of liquid nitrided high-speed steel (R6M5) at 560 °C for 40 min in a urea- Na_2CO_3 eutectic salt bath. The image reveals distinct ϵ -Fe₂₋₃N and γ' -Fe₄N compound layers with a diffusion zone of approximately 0.13 mm and a martensitic substrate beneath. Magnification: 2500 \times .

Figure 5 presents the cross-sectional SEM micrograph of the liquid nitrided high-speed steel (R6M5) sample processed at 560 °C for 40 min in a eutectic urea- Na_2CO_3 salt bath. The microstructural features clearly reveal the formation of a dense white layer at the top surface. Under higher magnification, distinct $\epsilon\text{-Fe}_{2-3}\text{N}$ and $\gamma'\text{-Fe}_4\text{N}$ compound layers can be observed, forming a diffusion zone of approximately 0.13 mm. This bright, compact surface layer — commonly referred to as the “white layer” — is characteristic of iron nitride phases typically produced during liquid nitriding, ensuring high surface hardness and wear resistance.

4. Discussions

The results of this study show that liquid nitriding at 560°C for 40 min significantly improved the performance of high-speed steels. The measured surface hardness of 1250-1300 HV and the diffusion depth of 0.10-0.16 mm are comparable to or in some cases superior to many previously reported studies. For example, Petrova et al. reported that the hardness level for gas-nitrided GSS after 10-20 h of treatment was only (1000-1150 HV), while several scientists have pointed out the inefficiency of conventional gas nitriding. Similarly, Gonzalez-Pochino et al. showed that plasma nitriding can achieve hardness values (1100-1250 HV) and excellent wear resistance, but the high energy consumption and expensive equipment of this process have limited its industrial application. Berladir et al. have studied liquid nitriding in the laboratory and have reported hardness values of around 1200 HV; however, since their work was not tested on an industrial scale, we can see that questions about scalability remain unanswered.

(AGMK) Industrial tests and studies conducted at the Almalyk Mining and Metallurgical Combine confirmed that the liquid nitriding apparatus extends its service life by 30-40% and reduces production costs by 15-20%. The findings provide strong evidence of the economic feasibility of this technique. In addition, the intervals for re-grinding nitrided tools were extended by 25-30%, which directly reduced the downtime in production. Such industry-approved benefits are rarely found in the literature, and this research will make a new contribution to this field [12-16].

From the point of view of energy efficiency, liquid nitriding is also useful. Compared to a few hours for nitriding plasma or gas, the process takes only (20-60) minutes. This leads to a 2-3-fold reduction in energy consumption, which makes it attractive for large-scale deployment. Moreover, the requirements for simple liquid nitriding equipment further reduce capital investments compared to plasma systems.

Comparison with the literature in the research process shows that liquid nitriding provided a unique balance of technical and economic advantages, achieving the same hardness and wear resistance as plasma nitriding, surpassing gas nitriding, and providing proven industrial advantages in terms of costs, equipment lifespan, and energy efficiency. This determines liquid nitriding as a competitive and expanding surface engineering method for high-speed steel milling machines [17-21].

A comparative assessment of the nitriding methods shows us that each method has its own advantages, as well as limitations. The general purpose of nitriding is to increase the hardness of the surface, wear resistance, and abrasion resistance, thereby extending the service life of the tool. The three most common approaches - gas nitriding, plasma nitriding, and liquid nitriding are summarized in table 5.

Table 5. Comparative analysis of nitriding methods

Method	Temp (°C)	Cycle Time	Surface HV	Pros	Cons
Gas nitriding	500–580	6–20 h	900–1200	Controlled CP	Long cycles
Plasma nitriding	450–550	4–12 h	1000–1300	High quality	Complex, costly
Liquid nitriding	540–580	20–60 min	1200–1300	Fast, uniform, low cost	Bath handling

Industrial experiments conducted at the Almalyk Mining and Metallurgical Combine give a clear idea of the economic and technical advantages of liquid nitriding technology over traditional heat treatment. The analysis focused on three main performance indicators: production costs, tool life and operating time [22-25].

- Tool service life: The service life of milling cutters undergoing liquid nitriding technology for 40

minutes at a temperature of 560 °C increased by 30-40% compared to traditional heat-treated tools. This improvement leads to an increase in the re-threading interval, a reduction in downtime, and stabilization of cutting productivity.

- Production costs: Due to the reduction in cycle time and energy consumption, the technology of liquid nitriding made it possible to reduce overall production costs by approximately 15-20%. The

reduction in costs led to significant consequences, especially in large-scale production, where savings made it possible to directly influence profitability.

- Cycle time: traditional heat treatment serves as the main one, but liquid nitriding technology sharply reduces the processing time from a few hours (typical for gas and plasma nitriding) to only 20-60 minutes. Such a shorter cycle allows for increased production efficiency and more flexible production schedules.

In general, cost-benefit analysis shows that liquid nitriding technology can combine high efficiency with significant economic benefits (table 6). Along with extending the service life of instruments, significant cost savings, and faster rotation, liquid nitriding technology is strategically advantageous and very important for industrial application at AMMC and similar large facilities.

Table 6. Cost-benefit analysis

Metric	Conventional HT	Liquid nitriding	Delta
Tool life (relative)	1.0	1.3–1.4	+30–40%
Production cost	100%	80–85%	–15–20%
Cycle time	Baseline	Short	Reduced

5. Conclusions

In this study, the process of liquid nitriding of high-speed steels R6M5 and R9F5 was systematically studied, and the possibility of its application in the production of milling cutters on an industrial scale was considered and evaluated. The main conclusions can be summarized as follows:

Improved process parameters. The technology of liquid nitriding at a temperature of 560 °C for 40 minutes provided the most favorable and perfect balance between hardness, growth of the diffusion layer, and processing efficiency. Under these conditions, a hardened layer of 0.10-0.15 mm with a surface hardness of 1250-1300 HV was obtained.

Compared to conventional heat treatment, the wear depth in liquid-nitrogenated samples decreased by 30-35%, and the coefficient of friction significantly decreased (from 0.62 to 0.44). These results confirm the formation of dense and stable nitride phases (γ' -Fe₄N and ϵ -Fe₂-3N), which significantly increases tribological indicators.

Comparison with alternative methods of nitriding technology. While gas nitriding technology requires a long processing cycle 6-20 hours and provides only moderate hardness plasma nitriding technology offers high-quality layers but while it is extremely expensive and complex liquid nitriding demonstrates a unique balance short processing time 20-60 minutes high hardness values, and economic scalability.

Industrial testing, testing, and cost. Experiments conducted at AGMK confirmed that the use of liquid nitriding technology for milling cutters increases the resource from a special tool by 30-40% and reduces production costs by 15-20%. This provides convincing evidence of the expediency and attractiveness of widespread application of the method.

Scientific and practical contribution. Outside the laboratory, this eliminates the difference between academic research and industrial practice. The innovation consists in combining microstructural mechanical and economic analyses to demonstrate that liquid nitriding technology is not only technically competitive but also industrially sustainable.

In conclusion, the technology of liquid nitriding can be recommended as a surface engineering technology, which is an important advantage for tools made of high-speed steel. Short processing time, cost-effectiveness, and industrial indicators make it a reliable alternative to gas and plasma nitriding. Future research should be focused on the automation of the process, the environmental aspects of processing molten salt, and the integration of liquid nitriding technology with hybrid surface engineering methods (for example, coatings or duplex processing) to further increase the efficiency and stability of instruments in modern production.

References

- [1] Peng, J., Wang, L., & Zhou, Y. (2019). The enhancement effect of salt-bath preoxidation on nitriding of steels. *Surface and Coatings Technology*, 374, 1189–1197. <https://doi.org/10.1016/j.surfcoat.2019.06.022>
- [2] González-Pociño, D., Berladir, K., & Stupak, V. (2024). Effects of nitriding and thermal processing on wear and tribological properties of tool steels. *Metals*, 14(2), 245. <https://doi.org/10.3390/met14020245>
- [3] Bonow, Vinicius & Maciel, Débora & Zimmer, André & Zimmer, Cínthia. (2019). Nitriding in low carbon steels using non-toxic salt baths. *Revista Liberato*. Pp: 177-186. <https://doi.org/10.31514/rliberato.2019v20n34.p177>
- [4] Wang, Y., & Xia, H. (2024). Investigation on microstructure, mechanical properties, and tribological behaviors of spray-formed high-vanadium high-speed steel after heat treatment. *Journal of Materials Engineering and Performance*, 33(4), 2019–2032. <https://doi.org/10.1007/s44251-024-00061-6>
- [5] Campos Becerra, L. H., Li, S., & Zhang, X. (2024). Influence of typical elements and heat treatment parameters on the hardenability of steels. *International Journal of Minerals, Metallurgy and Materials*, 31(7), 887–900. <https://doi.org/10.1007/s42243-024-01307-1>

- [6] Wang, Y., Zhang, C., & Liu, H. (2025). Heat treatment control technology of high-strength steel gears based on support vector machine. *Scientific Reports*, 15(1), 92312. <https://doi.org/10.1038/s41598-025-92312-1>
- [7] Xin, W., & Ling, J. (2023). Comparison and analysis on the effects of oil-quenching and salt-quenching for carburized gear rings. *Archives of Metallurgy and Materials*, 68(4), 1809–1820. <https://doi.org/10.24425/amm.2023.147882>
- [8] Shao, W., Liu, T., & Ren, J. (2022). Prediction and minimization of heat treatment induced distortion in drive gears. *Chinese Journal of Mechanical Engineering*, 35(1), 88. <https://doi.org/10.1186/s10033-022-00802-4>
- [9] Turk, M., & Kocaman, B. (2025). Investigation of the tribological and corrosion behavior of liquid-nitrided EN31 steel. *Turkish Journal of Engineering*, 9(2), 105–113. <https://doi.org/10.5152/turkijeng.2025.24067>
- [10] Hradil, David & Duchek, Michal & Hrbáčková, Taťána & Ciski, Aleksander. (2018). Gas nitriding with deep cryogenic treatment of high-speed steel. *Acta Metallurgica Slovaca*. 24. Pp: 187. <https://doi.org/10.12776/ams.v24i2.1058>
- [11] Bhadraiah, D. & Nouveau, C. & Boddu, Veeraswami & Rao, K. Ram Mohan. (2021). Plasma based nitriding of tool steel for the enhancement of hardness. *Materials Today: Proceedings*. 46. <https://doi.org/10.1016/j.matpr.2021.01.185>
- [12] Sagalovych, Alex and Popov, Viktor and Sagalovych, Vladislav and Dudnik, Stanislav and Bogoslavzev, Vladimir and Edinovych, Andrey. (2020). Comparative Analysis of the Fatigue Contact Strength of Surfaces Hardened by Cementation and the Ion Plasma Nitriding Avinit N (December 22, 2020). *Eastern-European Journal of Enterprise Technologies*, 6(12 (108)), 20-27, 2020. doi: <https://doi.org/10.15587/1729-4061.2020.217674>
- [13] Balıkcı, Ercan & Yaman, O. (2011). Investigation on liquid bath nitriding of selected steels. *Surface Engineering*. 27. Pp: 609-615. <https://doi.org/10.1179/1743294411Y.0000000034>
- [14] Petrova, L. (2022). Nitriding of High Speed Steel for Improvement of Tools Resistance. Pp: 204-208. <https://doi.org/10.21741/9781644901755-36>
- [15] Grün, R. & Voigtländer, D. (2009). Cost- and resource-efficient plasma-nitriding-based surface layer heat treatment for the gear-systems and tools industry, pp: 97-103.
- [16] Pantazopoulos, George & Papazoglou, T. & Antoniou, Stefanos & Sideris, J. (2003). Tribological Behaviour of a Liquid Nitrided Precipitation-Hardening (PH) Stainless Steel. *Materials Science Forum*. Pp: 1053-1058. <https://doi.org/10.4028/www.scientific.net/MSF>
- [17] Rakhadilov, Bauyrzhan & Kurbanbekov, Sherzod & Miniyaev, Arman. (2015). The influence of electrolytic-plasma nitriding on the structure and tribological properties of high-speed steels. *Journal "Tribologia"*, ISSN 0208-7774, (264). pp. 93- 104. 2015, Wrocław, Poland. Vol. 6. Pp: 93- 104.
- [18] Norkhudjayev, F. R., Mukhamedov, A. A., Guzashvili, K. V., Mirzarakhimova, Z. B., Shukurov, S. T., & Rizaeva, N. M. (2022). Investigation of the effect of special thermocyclic treatment on the defectiveness of the crystal structure of tool steels and their mechanical properties. *International Journal of mechatronics and Applied mechanics*, (12), Pp: 163-169.
- [19] Norkhudjayev, F. R., Mukhamedov, A. A., Tukhtasheva, M. N., Bektemirov, B. S., Shukurov Sh, T., & Gopirov, M. M. (2021). Influence of nitrocementation modes on the change in the hardness of the surface layer of structural steels. *JournalNX*, 7(11), Pp: 75-77.
- [20] Shahobiddin, S. (2025). Technology of strengthening teeth of milling cutter using liquid nitriding. *Universum: технические науки*, 8(4 (133)), Pp: 19-21.
- [21] Shukhrat Shakirov, Begali Bektemirov, Sanobar Sadaddinova, Ulugbek Umirov, Mukhlisakhon Abdurakhmonova, Kamoliddin Urokov, & Zukhra Mirzarakhimova. (2025). Mathematical Modelling Concerning Compressibility of Air In Porosity During Semi-Dry Pressing Process Of Ceramic Powder. *International Journal of Integrated Engineering*, 17(1), Pp: 1-16. <https://penerbit.uthm.edu.my/ojs/index.php/ijie/article/view/16171>
- [22] Shoirtdjan Karimov, Shukhrat Shakirov, Begali Bektemirov, Nuriddin Khusanov, Sherzod Mamirov; Determination of power balance of powder coating process using electrocontact method. *AIP Conf. Proc.* 15 July 2025; 3256 (1): 050007. <https://doi.org/10.1063/5.0266849>
- [23] Fayzullaev, J. S., Negmatov, S. S., Pirmatov, R. H., Negmatova, K. S., Abed, N. S., Ikramova, M. E. (2025). Development of technology for the production of hot-rolled heat-strengthened metal composite fittings of class A500C based on local and secondary raw materials. In *AIP Conference Proceedings* (Vol. 3286, No. 1, p. 060013). AIP Publishing LLC.
- [24] Rasulov, A., Alikulov, A., Djalolova, S., Tukhtasheva, M., Fayzullaev, A., & Sattarov, A. (2024). Manufacturing tools with a combination of strength and ductility using molybdenum powders. *International Journal of Mechatronics and Applied Mechanics*, (18), Pp: 216-221.
- [25] Sarvar, T., Nodir, T., Mardonov, U., Saydumarov, B., Kulmuradov, D., & Boltaeva, M. (2024). Effects of germanium (Ge) on hardness and microstructure of Al-Mg, Al-Cu, Al-Mn system alloys. *International Journal of Mechatronics and Applied Mechanics*, (16), 179-184. <https://doi.org/10.17683/ijomam/issue16.21>